

1 Title:

2 **Predicting diversity changes in subalpine moorland ecosystems based on geometry**
3 **of species distributions and realistic area loss**

4

5 A short running title:

6 **Diversity responses to realistic area loss**

7

8 Daichi Makishima^{a,†}, Naohiro Ishii^{a,b,†}, Rui Sutoh^a, Akihito Goto^a, Yutaka Kawai^c,
9 Hayami Taniguchi^c, Kei Uchida^{a,d}, Masaya Shimazaki^c, Tohru Nakashizuka^e, Yoshihisa
10 Suyama^b, Kouki Hikosaka^c, and Takehiro Sasaki^{a,*}

11

12 ^a Graduate School of Environment and Information Sciences, Yokohama National
13 University, 79-7 Tokiwadai, Hodogaya, Yokohama, Kanagawa 240-8501, Japan

14 ^b Field Science Center, Graduate School of Agricultural Science, Tohoku University,
15 232-3 Yomogida, Naruko-onsen, Osaki, Miyagi 989-6711, Japan

16 ^c Graduate School of Life Sciences, Tohoku University, Aoba, Sendai, Miyagi 980-
17 8578, Japan

18 ^d Institute for Sustainable Agro-ecosystem Services, The University of Tokyo, 1-1-1
19 Midori-cho, Nishitokyo, Tokyo 118-0002, Japan

20 ^e Forestry and Forest Products Research Institute, 1 Matsunosato, Tsukuba, Ibaraki 305-
21 8687, Japan

22

23 *** Corresponding author:** Takehiro Sasaki

24 **E-mail address:** sasaki-takehiro-kw@ynu.ac.jp

25 **Phone/Fax:** (+81)-45-339-3596

26

27 † DM and NI equally contributed to this work

28

29 **ORCID ID**

30 Takehiro Sasaki: <https://orcid.org/0000-0001-8727-9152>

31 Kouki Hikosaka: <https://orcid.org/0000-0003-1744-3775>

32 Yoshihisa Suyama: <https://orcid.org/0000-0002-3136-5489>

33

34 **Funding information**

35 This work was financially supported by a Fostering Joint International Research A (no.

36 19KK0393) and a Grant-in-Aid for Scientific Research B (no.18H02221 and no.

37 20H04380) to TS from the Ministry of Education, Culture, Sports, Science and

38 Technology of Japan.

39

40 **Abstract**

41 Question:

42 How does plant species richness respond to simulated area loss based on the realistic

43 geometry of area loss in subalpine moorland ecosystems?

44

45 Location:

46 Hakkoda mountain range, Aomori, Japan

47

48 Methods:

49 We constructed species distribution models based on relationships between species
50 distributions and environmental conditions in subalpine moorland ecosystems. We then
51 simulated moorland area loss based on the realistic geometry of area loss from the past
52 (1967) to the present (2019) to predict future changes in plant diversity. Here, we
53 defined the realistic geometry of area loss as the plausible spatial pattern of future
54 habitat loss. Finally, we analyzed how the rate of species loss in response to the realistic
55 area loss can be explained by a range of factors including spatial patterns in species
56 distributions, total number of species present, and environmental variables for the focal
57 moorland.

58

59 Results:

60 Within each moorland site, areas prone or those less prone to be lost were distributed
61 nonrandomly at a local scale. In general, the patterns of species loss caused by the
62 realistic area loss differed from those caused by random area loss. At most sites, the
63 realistic area loss caused a relatively small decline in species richness, until a certain
64 threshold of area loss and accelerating decline thereafter. None of the factors can
65 explain the rate of decrease in species richness caused by the realistic area loss. At the
66 species level, however, species with lower occurrence rates at a given site can be lost
67 earlier than those with higher occurrence rates by the realistic area loss.

68

69 Conclusions:

70 Patterns of habitat loss and species distributions are not spatially random, and the
71 classical species-area based approach assuming random area loss can thus either under-
72 or overestimate the risk of species loss.

73

74 **Keywords:** climate change; generalized additive model; global warming; historical

75 landscape; kriging; random forest

76 **Introduction**

77 Habitat loss and fragmentation have profound impacts on global biodiversity (Fahrig,
78 2003; Foley et al., 2005; Ibáñez et al., 2014) via species extinction and decreased local
79 species richness (Jamin et al., 2020; Noh et al., 2019; Olsen et al., 2018). Predicting
80 how species will be lost due to area loss is one of the most important issues in
81 biodiversity conservation, but much is still uncertain about the best approach to use (He
82 & Hubbell 2011). A classical approach to predict species loss is based on the
83 relationship between species richness and area, which has long been an important tool
84 for conservation planning (Koh & Ghazoul 2010; Pereira et al. 2010). The species
85 richness–area relationship assumes that species will be lost according to random area
86 loss and that inhabitant species in the focal area do not exhibit any spatial pattern.
87 However, because patterns of habitat loss and species distributions are not spatially
88 random, the classical approach can either under- or overestimate the risk of species loss
89 (Deane et al., 2017; De Camargo et al., 2015; He and Hubbell, 2011; Keil et al., 2015).
90 Therefore, to more accurately predict species loss in response to habitat area loss, we
91 need to account for actual species distributions and how areas are lost in a given habitat
92 (Keil et al. 2015).

93 In assessing species distributions across a large area, species distribution modeling
94 (SDMs; Elith et al., 2011; Merow et al., 2013; Williams et al., 2021) can serve as an
95 efficient alternative to field-based investigations. SDMs can estimate the probability of
96 species' occurrence using the relationships between species presence (and absence) and
97 environmental variables at locations where species are present (and absent). SDMs are
98 widely used in conservation biology; for example, species loss or invasion can be
99 predicted by substituting climate change scenarios and projected future environmental

100 changes into the SDMs (Shimazaki et al. 2012; Zhang et al. 2017; Williams et al. 2021).
101 SDMs are often based on data of species occurrence and environmental conditions at a
102 coarse resolution (i.e., $>1 \text{ km}^2$; Williams et al., 2021; Zhang et al., 2017), but can be
103 applied to predict species presence and/or absence at a fine resolution as long as such
104 data are available at a fine scale (Shimazaki et al. 2012).

105 In real ecosystems, habitat loss and fragmentation always occur nonrandomly
106 regardless of whether they are anthropogenically or naturally induced (Deane et al.,
107 2017; He and Hubbell, 2011; Keil et al., 2015). In a study of three taxa in nine regions
108 across four continents, Keil et al. (2015) demonstrated that inward loss of habitats leads
109 to more pronounced declines of species richness than when habitats are lost from the
110 inside toward the edges or are lost randomly. Their models indicate that this can happen
111 for at least two reasons. First, species' ranges may be nonrandomly concentrated close
112 to the edges for ecological reasons, for example, because of the presence of suitable
113 habitats in those areas. Second, the higher relative impact of inward area loss is
114 expected in randomly distributed contiguous ranges, when the ranges are truncated or
115 cropped by region boundaries. However, these estimates of diversity loss were still
116 based on defined and contiguous forms (inward vs. outward area loss) and not on
117 realistic geometry of habitat area loss (Keil et al. 2015). Here, we defined the realistic
118 geometry of habitat area loss as the plausible spatial pattern of future habitat loss. In
119 subalpine moorland ecosystems in Japan, Makishima et al. (2021) used past (in 1967)
120 and present (in 2019) aerial photographs to identify spatial features of moorlands and
121 their long-term changes. By overlaying present photographs on past ones, the authors
122 revealed a spatial bias in the way the areas decreased within the focal moorland. We
123 assumed that the locations with more decreasing areas from the past to the present are

124 those where area loss will be relatively more likely to occur in future. Through spatial
125 interpolation of fine-scale area loss patterns, we quantified the realistic geometry of
126 moorland area loss.

127 Here, to predict species loss due to realistic habitat area loss, we combined the
128 construction of SDMs to predict fine-scale extensive distributions of present species
129 with simulations of area loss based on the realistic geometry of area loss in subalpine
130 moorland ecosystems in Japan. The moorland ecosystem is one of the most vulnerable
131 to environmental changes and habitat loss and fragmentation (Chapin et al., 2000;
132 Daimaru and Yasuda, 2009; Kudo et al., 2017; Sasaki et al., 2014). Indeed, many
133 mountainous moorlands in Japan are losing area rapidly (Geospatial Information
134 Authority of Japan, 2000), despite being subjected to few direct human disturbances,
135 and moorland specialist species are at risk of local extinction (Jamin et al. 2020).
136 Although previous studies suggested that habitat specialists are sensitive to habitat loss
137 and fragmentation and associated environmental changes (e.g., Henle et al., 2004), there
138 might be considerable differences in species loss patterns depending on how specialist
139 as well as generalist species are distributed and how area is lost (Jamin et al., 2020;
140 Olsen et al., 2018). Therefore, in this study we aimed to quantify the responses of
141 species richness of all species, moorland specialists, and generalists to simulated area
142 loss. To do this, we first constructed SDMs based on the relationships between present
143 species distributions and a range of environmental variables. Second, we performed
144 moorland area loss simulations based on the realistic geometry of area loss from the past
145 (1967) to the present (2019) to predict how species will be lost in the future. Finally, we
146 analyzed how the rate of species loss according to simulated area loss based on the
147 realistic geometry of area loss can be explained by a range of factors including spatial

148 patterns in species distributions, total number of species present, and environmental
149 variables for the focal moorland.

150

151 **Methods**

152 *Study area and sites*

153 The study area is located in the Hakkoda mountain range (peak coordinates: 40°41'N,
154 140°52'E, 1584 m a.s.l.) in Aomori Prefecture, northern Japan (Fig. S1). The annual
155 maximum snow depth, mean temperature, and precipitation between 2009 and 2018
156 ranged from 3 to 6 m, 5 to 6 °C, and 1600 to 2200 mm, respectively, at the Sukayu
157 meteorological station (40°38.9'N, 140°50.9'E).

158 We selected nineteen moorland sites based on their physical accessibility and
159 gradients of physical characteristics of moorlands, including their area size and spatial
160 configuration, as well as environmental factors including elevation, temperature, pH,
161 and electric conductivity (EC)(Makishima et al. 2021). In this study, taxonomic
162 nomenclature follows the YList (BG Plants index: <http://ylist.info/index.html>).

163 The study area is a conservation reserve (Towada-Hachimantai National Park), and
164 therefore human impacts on natural vegetation have been minimal. Nonetheless, within
165 the study area, habitat loss and fragmentation of the moorlands are progressing rapidly,
166 and the areas of the 19 studied moorlands have decreased by an average of 50.01% over
167 the past ~50 years (Makishima et al. 2021). Even if direct human impacts are minimal,
168 earlier snowmelt in spring associated with recent climate change may facilitate
169 expansion of shrubby species, leading to habitat loss and fragmentation of mountainous
170 moorlands in Japan (Kudo et al. 2017). The causes remain unexplored, however, and
171 need to be studied by using long-term observation data. Other general descriptions of

172 the study area and sites have been provided by Sasaki et al. (2013) and Makishima et al.
173 (2021).

174

175 *Vegetation sampling*

176 We sampled vegetation along six 20-m transects, separated evenly by at least 20 m
177 (range 20–200 m) within each moorland site, and laid out five quadrats of 1×1 m on
178 each transect at intervals of 5 m, for a total of 570 quadrats along 114 transects sampled
179 at 19 sites (Makishima et al. 2021). In August 2018, the coverage of each species in
180 each quadrat was visually estimated by the first, second, and third authors (to ensure
181 consistency) using a modified Daubenmire percent cover scale (Daubenmire, 1959): 1,
182 $\leq 1\%$; 2, 2–5%; 3, 6–25%; 4, 26–50%; 5, 51–75%; 6, 76–95%; 7, $>95\%$. In this study,
183 however, we used presence/absence information of present species across quadrats. To
184 construct the SDM (see section 2.5), only the cover of *Sphagnum* spp. was determined
185 by converting Daubenmire scores to the midpoint of the percentage range spanned by
186 each score (e.g., a score of 5 was converted to 63% cover). Seventy-two vascular plant
187 species were recorded across the entire landscape. Consequently, we compiled a
188 species-by-quadrat matrix for the following analyses. Moorland specialist species were
189 defined based on descriptions of Japanese flora (Satake et al., 1982, 1989).

190

191 *Environmental data*

192 We measured soil moisture (%), pH, and EC (as a surrogate for salinity; $\mu\text{S cm}^{-1}$) of the
193 soil solution close to each quadrat ($n = 570$) using digital soil moisture (DIK-311F;
194 Daiki Rika Kogyo Co., Ltd., Saitama, Japan), pH, and EC meters (pH-22B and B-173;
195 HORIBA Ltd., Kyoto, Japan), respectively, in August 2018. We measured soil moisture

196 at least 3 days after the last precipitation event at each site. Gradients in soil moisture,
197 pH, and EC are known to be primary factors contributing to vegetation patterns in
198 subalpine moorland ecosystems (Gorham et al., 1984; Wheeler and Proctor, 2000). We
199 averaged the soil moisture, pH, and EC across quadrats within each site.

200 To construct the SDM based on the relationships between species composition and
201 environmental variables at the quadrat level (see section 2.5), we divided the present
202 site area into 20×20 m or 40×40 m grids (depending on the site area; Table 1) using
203 ArcGIS (version 10.6, ESRI, Redlands, CA, USA) and measured the environmental
204 variables within each grid. We varied the size of grids among sites to optimize our
205 sampling efforts (i.e., if we use of 20×20 m grids for larger sites, we need enormous
206 sampling efforts). Based on the present (2019) aerial photograph (see section 2.4), the
207 grids were created to cover the area of each moorland site and then clipped by the
208 polygon of each site (Fig. S2). The grids inside the site perimeter in 2019 that were
209 covered mostly or completely by trees were also measured. However, the grids
210 completely outside the site perimeter in 2019 were not measured even when the grids
211 were inside the site perimeter in 1967. We measured soil moisture, pH, EC, and the
212 cover of *Sphagnum* spp. (hereafter, *Sphagnum* cover) at three random points to account
213 for environmental heterogeneity in each grid. *Sphagnum* cover was recorded using a
214 modified Daubenmire percent cover scale (Daubenmire, 1959), and Daubenmire scores
215 were then converted to the midpoint of the percentage range spanned by each score. The
216 same equipment was used for pH, EC, and soil moisture content measurements as noted
217 above. Environmental measurements for each grid at each site were performed in
218 August 2019.

219

220 *Spatial parameters*

221 The perimeters of all moorlands within the study area were first delineated through
222 visual interpretation of the past (1967) and present (2019) aerial photographs and then
223 digitally mapped using ArcGIS. For details on the digitization of photographs, see
224 Sasaki et al. (2012). In both periods, we estimated the area of each grid excluding area
225 covered by trees.

226 We then calculated the natural logarithm of the difference between past and present
227 area for each grid (log difference; LD):

$$228 \quad LD = \ln A' - \ln A = \ln \left(\frac{A'}{A} \right), \quad (1)$$

229 where A and A' represent the area of the focal grid in 1967 and in 2019, respectively.

230 From the present aerial photographs, we derived a set of spatial parameters for each
231 grid, including elevation and distance to the moorland perimeter. Within-site scale
232 variations in elevation (i.e., microtopography) can contribute to plant species
233 distribution in moorland ecosystems (Hájková et al. 2006; Sasaki et al. 2013). In
234 addition, previous studies reported that moorland edges often have less soil moisture
235 than the interior, leading to the formation of community composition specific to
236 moorland edges (Merlin et al. 2015; Boughton et al. 2021). We therefore calculated the
237 nearest distance from the moorland edge to the center of each quadrat along vegetation
238 survey transects and each grid. However, when the center of a grid (the center of each
239 quadrat was never outside of the perimeter) was outside of the moorland perimeter, the
240 nearest distance from the edge was set to zero.

241

242 *Species distribution models*

243 To predict the species presence and absence at each grid at each moorland site based on

244 environmental conditions at each grid, SDMs were constructed using three types of
245 statistical models: a generalized linear mixed-effects model (GLMM), a generalized
246 additive mixed-effects model (GAMM), and random forests. We did not use alternative
247 methods based on presence-background modeling such as Maxent (Phillips et al. 2006)
248 because Maxent was not originally programmed to incorporate species presence-
249 absence information, and using Maxent seems circuitous even though such information
250 is available (Guillera-Arroita et al. 2014).

251 First, to clarify the relationships between species distribution and environmental
252 conditions, we used the field-based data at the survey quadrat level. In selecting
253 explanatory variables, since the measured soil moisture and *Sphagnum* cover showed a
254 weak positive correlation ($p < 0.001$, $r = 0.22$), soil moisture was omitted, and
255 *Sphagnum* cover was selected as an explanatory variable because it is considered to
256 have relatively small temporal variation compared to that of soil moisture. Accordingly,
257 the response variable for the three statistical models was the presence/absence (0/1) of
258 each plant species present across the quadrats ($N = 570$; i.e., three SDMs were
259 constructed for each present species across the studied area), and the explanatory
260 variables were elevation, pH, EC, *Sphagnum* cover, and distance from the moorland
261 edge. In the GLMM and GAMM, we used a binomial error structure and a logit link
262 function. We also incorporated the ID of each moorland site as a random effect in the
263 GLMM and GAMM.

264 Next, for each species, we selected the best-fit model and verified its accuracy. For
265 model selection, among the three SDMs (GLMM, GAMM, and random forest), we
266 evaluated which model provided the best fit by using the area under the curve (AUC),
267 which takes values from 0 to 1. An AUC of 0.5 means that the model prediction is

268 random, $0.6 < \text{AUC} < 0.7$ means that the accuracy of the model is low, $0.7 \leq \text{AUC} < 0.8$
269 means that the accuracy is moderate, and $0.8 \leq \text{AUC} \leq 1.0$ means that the accuracy is
270 high (Manel et al., 2001; Pearce and Ferrier, 2000). For each species, the model with the
271 highest AUC value among the three SDMs was adopted as the SDM for that species
272 (note that selected SDMs were GLMM for all species; Table 2). Species with $\text{AUC} < 0.6$
273 in any of the three models were excluded from subsequent analyses. In addition to the
274 AUC, the accuracy of the models was confirmed by comparing predicted data with the
275 measured data (i.e., cross-validation). We randomly divided the data ($N = 570$) of all
276 quadrats in half ($N = 285$) and used half of the data (training data) to build prediction
277 models for each species. The models used in the cross-validation were those selected by
278 AUC. Then, the models were used to predict the presence/absence of each species based
279 on environmental conditions in the other half of the data that was not used in the
280 prediction models. The threshold for determining presence/absence was set at 0.5;
281 species were assigned presence if the model predicted a value greater than 0.5 and
282 absence if the model predicted a value less than 0.5. The predicted presence/absence
283 information of the species was compared with the actual occurrence of the species, and
284 the accuracy rate was calculated. This process was repeated 1000 times, and the
285 accuracy rate was averaged to confirm the cross-validation of SDMs for each species.
286 SDMs with $\text{AUC} > 0.6$ but with a mean accuracy rate $< 60\%$ were excluded from
287 further analysis. We also excluded from the analysis species for which the number of
288 occurrences across the quadrats was too small for us to calculate a robust accuracy rate.

289 Following these procedures, we predicted the presence/absence of each species at
290 each grid at each moorland site based on the environmental conditions of each grid
291 using the SDMs. Our SDMs can be applied for 30 species (see Results for details).

292

293 *Quantifying the likelihood of grid-based area loss*

294 We used universal kriging to perform areal smoothing of the likelihood of area loss at
295 the grid level. We defined the likelihood of area loss based on LD, that is, the grids with
296 smaller LD (more decreasing areas from the past to the present) are the locations at the
297 focal moorland where area loss will be relatively more likely to occur. In this study, the
298 LD of each grid was spatially interpolated by kriging to estimate the areal LD within the
299 moorland site. The areal LD estimates were then averaged for each grid and ordered
300 based on the average LD values, which were used for the simulation rules (grids with
301 lower LD estimates were more likely to be lost earlier).

302

303 *Grid-based area loss simulations*

304 Based on the likelihood of area loss for each grid, we simulated the sequential loss of
305 grids to examine how species are lost. This grid-based area loss simulation was run until
306 all grids at the moorland site were lost. Such consequences of simulated area loss based
307 on the realistic area loss were compared with those of randomly simulated area loss. In
308 that case, a grid was randomly lost at each site, and we repeated 1000 sets of random
309 area loss simulations until all grids were lost. The trajectory of change in species
310 richness of all species, moorland specialists, and generalists according to the simulated
311 area loss was visualized for each site. In the area loss simulation based on the realistic
312 geometry of area loss, we summarized the proportion of area lost leading to local
313 extinction of each species across the sites.

314

315 *Exploring the factors determining the rate of species loss according to simulated area*

316 *loss based on the realistic geometry of area loss*

317 We explored how the rate of species loss according to the realistic area loss can be
318 explained by a range of factors including spatial patterns in species distributions, initial
319 species richness (total number of species present before simulated area loss), and
320 environmental variables for the focal moorland. We first defined the half-life of species
321 richness, as a rate of decreasing species richness due to the realistic area loss, calculated
322 as the area that must be lost to halve the initial species richness divided by the original
323 area at each site. The half-life of species richness close to 0 means a shorter half-life,
324 whereas that close to 1 means a longer half-life.

325 For quantifying spatial patterns in species distributions, we used Clark and Evans'
326 aggregation index (Clark and Evans 1954). This aggregation index uses the observed
327 mean nearest-neighbor distances and the expected nearest-neighbor distances under
328 complete spatial randomness in species distribution. Ratios of observed to expected
329 mean nearest-neighbor distances below 1 indicate clustering, values greater than 1
330 uniformity. If a species is predicted by SDM to be present in a given grid at each site,
331 the location of species is fixed for the centroid of that grid. For each species, we
332 computed the distances from all centroids where species are present to their nearest
333 neighbors, and averaged the values of aggregation index across species.

334 In addition to area and elevation, we quantified the indices of isolation and
335 moorland shape as environmental variables describing the focal moorland. We
336 quantified the isolation index as suggested by previous studies (see Hanski et al. 1994;
337 Sasaki et al. 2012, for details). Larger values of this index indicate less isolation than
338 smaller values. The shape index was calculated as perimeter divided by area of the focal
339 moorland.

340 We used a generalized linear model with a binomial error structure and logit link to
341 analyze the relationship between the half-life of species richness, and initial species
342 richness, averaged aggregation index across species, area, isolation, and elevation at
343 each site. We excluded the shape index from this model to avoid a multicollinearity
344 problem. In addition, we regressed the proportion of area lost leading to local extinction
345 of each species against aggregation index and occurrence rate (number of predicted
346 occurrences divided by number of grids at each site) of each species at each site, by
347 using a generalized linear mixed-effects model with a binomial error structure and logit
348 link. Phylogenetic constraints were controlled by adding family as a random effect in
349 the model. Because we varied the size of grids among sites (20×20 m or 40×40 m
350 grids), we repeated these analyses by using the subset data from the sites with a 40×40
351 m grid resolution as well as that from the sites with 20×20 m grid resolution (see Table
352 1).

353 All data analyses were performed with R software (version 4.0.3; R Development
354 Core Team, 2020) using the “`gamm4`,” “`lme4`,” “`randomForest`,” “`car`,” “`vegan`,”
355 “`pROC`,” and “`ROCR`,” “`spatstat.core`” packages.

356

357 **Results**

358 Our SDMs (i.e., models with $AUC > 0.6$ and accuracy $> 60\%$) predicted the
359 distributions of 30 species of a total of 72 species identified across the survey quadrats.
360 Of a total of 72 species, 38 were moorland specialists and 34 were generalists (Table
361 S1). Of 30 species predicted by the SDMs, 22 were moorland specialists and 8 were
362 generalists (Table 2). The mean AUC score of the 30 SDMs was 0.915, and the mean
363 accuracy was 86.3% (Table 2). AUC score and accuracy were significantly positively

364 correlated (Figure S3). Among the 30 species, those with the highest predicted rate of
365 occurrence across grids were *Moliniopsis japonica*, *Vaccinium oxycoccos*, and *Drosera*
366 *rotundifolia* (in this order). In general, species with higher occurrence rates across the
367 quadrats were predicted to occur in most grids (Fig. S4). For some species, however,
368 such as *Trientalis europaea* and *Helonias orientalis*, the rate of predicted occurrences
369 across grids was lower than the actual rate of occurrences across the quadrats. The
370 degree of spatial aggregation/disaggregation in the predicted distribution differed among
371 each species (Fig. 1). Similarly, we noted that the predicted species richness is spatially
372 heterogeneous within each site (Fig. 2b, c, e, f, h, i), and there is also a spatial
373 heterogeneity in the likelihood of grid-based area loss within a site (Fig. 2a, d, g).

374 In general, the patterns of species loss caused by simulated area loss based on the
375 realistic area loss deviated from those caused by randomly simulated area loss (Fig. 3;
376 the 95% CIs for species loss trajectories by random area loss did not generally overlap
377 with species loss trajectories by realistic area loss). At most sites, realistic area loss
378 caused a relatively small decline in species richness, until a certain threshold of area
379 loss and accelerating decline thereafter. At fewer sites (Shimokenashi C, Tamoyachi A,
380 and Takada B sites), realistic area loss caused an approximately proportional decrease in
381 species richness. The effects of simulated area loss on all 30 species (including
382 moorland specialist species) were generally similar when we focused on only moorland
383 specialist species (Fig. 4) or generalist species (Fig. 5). We further visualized the
384 proportion of area lost leading to local extinction of each species across moorland sites
385 (Fig. 6), and the proportion varied among species as well as moorland sites.

386 None of the factors can explain the half-life of species richness (Table 3). This was
387 probably due to the robust responses of species richness to realistic area loss (i.e., the

388 half-life of species richness was biased to a high value; Fig. S5). At the species level,
389 however, species with lower occurrence rates at a given site can be lost earlier than
390 those with higher occurrence rates by realistic area loss (Table 4). These results were
391 consistent when we used the subset data from the sites with a 40×40 m grid resolution
392 as well as that from the sites with 20×20 m grid resolution (Tables S2 and S3).

393

394 **Discussion**

395 Based on the simulation of possible area loss at each site, we found that the patterns of
396 species loss caused by the realistic area loss generally deviated from those caused by
397 random area loss (Fig. 3). At most sites, realistic area loss caused a relatively small
398 decline in species richness, until a certain threshold of area loss and accelerating decline
399 thereafter. At fewer sites (Shimokenashi C, Tamoyachi A, and Takada B sites), realistic
400 area loss caused an approximately proportional decrease in species richness. These
401 findings on the effects of simulated area loss on all 30 species (including moorland
402 specialist species) were similar when we focused only on moorland specialist species
403 (Fig. 4) or generalist species (Fig. 5). The half-life of species richness, a rate of
404 decreasing species richness due to realistic area loss, could not be explained by initial
405 species richness, averaged aggregation index across species, area, isolation, and
406 elevation at each site (Table 3). This result was probably due to that the half-life of
407 species richness did not vary substantially among sites and was rather biased to a high
408 value (Fig. S5).

409 Previous studies have suggested that habitat specialist species (in our case, moorland
410 specialist) are sensitive to habitat loss and fragmentation and associated environmental
411 changes (Henle et al., 2004; Jamin et al., 2020; Olsen et al., 2018). Depending on how

412 specialist species are distributed and how area will be lost, however, there might be
413 considerable differences in patterns of species loss (Jamin et al., 2020; Olsen et al.,
414 2018). Our species-level analysis (Table 4) revealed that species with lower occurrence
415 rates at a given site can be lost earlier than those with higher occurrence rates by
416 realistic area loss. Relatively rare species such as *Coptis trifolia*, *Menyanthes trifoliata*,
417 *Carex michauxiana*, *Rhododendron molle* subsp. *japonicum*, and *Platanthera tipuloides*
418 will be lost earlier, whereas relatively abundant species such as *Moliniopsis japonica*,
419 *Eriophorum vaginatum*, and *Narthecium asiaticum* will be lost later in the face of
420 possible area loss (Fig. 6). The proportion of area lost leading to local extinction thus
421 varied substantially among species and moorland sites, suggesting that area loss and
422 species loss do not occur uniformly (Keil et al. 2015) and that the patterns of species
423 loss would depend on the actual species distribution and how the area is lost in a focal
424 moorland. Furthermore, the realistic geometry of area loss indicated that possible area
425 loss would not necessarily occur from the edge of a focal moorland (Fig. 2), and non-
426 moorland specialist species (which are likely to be distributed along moorland edges)
427 will not necessarily be lost earlier than moorland specialists due to realistic area loss
428 (Fig. 6). Therefore, it appears that our results are not an artifact of such edge effects.

429 Our grid-based area loss simulations assumed no environmental changes,
430 microhabitat shifts of present species, or colonization of new species (especially shrub
431 encroachment) associated with area loss. Thus, our simulations might overestimate
432 species loss due to possible area loss of moorlands. The impacts of moorland area loss
433 on subsequent environmental changes within a moorland and potential microhabitat
434 shifts and colonization, if any, need to be carefully monitored in the future. Nonetheless,
435 the sites with greater rates of species loss based on simulated possible area loss rather

436 than on random area loss are of conservation concern. In those cases where rapid
437 species loss with possible area loss would lead to a rapid decline in functioning and
438 persistence of a given community (Sasaki et al. 2014), such communities would be of
439 highest concern. At moorland sites located at higher elevations, including Kamikenashi
440 A, Kamikenashi B, Shimokenashi B, Shimokenashi C, Tamoyachi A, and Suiren A,
441 rapid species loss due to possible area loss would be paralleled with a rapid decline in
442 functional diversity (Sasaki et al. 2014) as a surrogate for functioning and persistence of
443 communities.

444 Our SDMs had relatively high AUC scores and accuracy rates, suggesting that they
445 were able to accurately predict the spatial distributions of the 30 species (Table 2; Fig.
446 S3). Ideally, if we had more fine-scale grids and measured more environmental
447 variables regulating species presence/absence (particularly hydrological states such as
448 groundwater level), we might be able to predict more species and increase the model
449 accuracy (Elith et al. 2011). Because we needed to extensively survey multiple
450 moorland sites, we selected environmental variables that could be easily and rapidly
451 measured at a reasonably fine scale (20×20 m or 40×40 m grids). As a result, we may
452 have missed some important responses of species to moorland area loss (Fig. 6), but we
453 believe that our SDMs and area loss simulations track well the relative rates of species
454 diversity change according to possible area loss in the future.

455 In this study, we predicted diversity changes in subalpine moorland ecosystems
456 based on spatial patterns in species distributions and moorland area loss. The
457 assumptions of the classical approach based on the species richness–area relationship
458 that species are lost proportionally to area loss and that inhabitant species in the focal
459 area do not exhibit any spatial pattern may not hold in most cases (Deane et al., 2017;

460 De Camargo et al., 2015; He and Hubbell, 2011). As demonstrated in our study, patterns
461 of habitat loss and species distributions are not spatially random, meaning that the
462 classical approach can either under- or overestimate the risk of species loss. When
463 predicting the risk of local extinction due to habitat loss and fragmentation in
464 ecosystems in general, we recommend incorporating both actual species distributions
465 and possible spatial patterns of area loss (He & Hubbell 2011; Keil et al. 2015).

466

467 **Acknowledgements**

468 We thank our laboratory members for helping with field work, especially Yuki
469 Iwachido, Misa Nambu, Issei Nishimura, and Yutaro Yoshitake. Two anonymous
470 referees and Shin-ichi Tatsumi contributed significantly to the clarity of the manuscript.

471

472 **Authors' contributions**

473 DM, NI, and TS conceived of and designed the study. All authors collected the data.
474 DM and NI analyzed the data. DM and TS wrote the first draft of the manuscript, and all
475 authors contributed to revisions. DM and NI equally contributed for this manuscript.

476

477 **Data accessibility**

478 The data supporting the result in the paper will be archived in figshare at the time of
479 acceptance and the data DOI will be included.

480

481 **REFERENCES**

482 Boughton, E.H., Quintana-Ascencio, P.F., & Bohlen, P.J. 2021. Grazing and
483 microhabitat interact to affect plant–plant interactions in subtropical seasonal

- 484 wetlands. *Journal of Vegetation Science* 32: e12962.
- 485 De Camargo, R.X., Currie, D.J., & Morris, D.W. 2015. An empirical investigation of
486 why species-area relationships overestimate species losses. *Ecology* 96: 1253–
487 1263.
- 488 Chapin, F.S., Mcguire, A.D., Randerson, J., Pielke, R., Baldocchi, D., Hobbie, S.E.,
489 Roulet, N., Eugster, W., Kasischke, E., Rastetter, E.B., Zimov, S.A., & Running,
490 S.W. 2000. Arctic and boreal ecosystems of western North America as components
491 of the climate system. *Global Change Biology* 6: 211–223.
- 492 Clark, J., & Evans, F.C. 1954. Distance to nearest neighbour as a measure of spatial
493 relationships in populations. *Ecology*, 35: 445–453.
- 494 Daimaru, H., & Yasuda, M. 2009. Global warming and mountain wet meadows in
495 Japan. *Chikyu Kankyo* 14:175–182. (in Japanese)
- 496 Daubenmire, R.F. 1959. Canopy coverage method of vegetation analysis. *Northwest Sci*
497 33:43–64
- 498 Deane, D.C., Fordham, D.A., He, F., & Bradshaw, C.J.A. 2017a. Future extinction risk
499 of wetland plants is higher from individual patch loss than total area reduction.
500 *Biological Conservation* 209: 27–33.
- 501 Deane, D.C., Fordham, D.A., He, F., & Bradshaw, C.J.A. 2017b. Future extinction risk
502 of wetland plants is higher from individual patch loss than total area reduction.
503 *Biological Conservation* 209: 27–33.
- 504 Elith, J., Phillips, S.J., Hastie, T., Dudík, M., Chee, Y.E., & Yates, C.J. 2011. A
505 statistical explanation of MaxEnt for ecologists. *Diversity and Distributions* 17:
506 43–57.
- 507 Fahrig, L. 2003. Effects of Habitat Fragmentation on Biodiversity. *Annu Rev Ecol Evol*

- 508 Syst 34:487–515.
- 509 Foley, J.A., DeFries, R., Asner, G.P., Barford, C., Bonan, G., Carpenter, S.R., Chapin,
510 F.S., Coe, M.T., Daily, G.C., Gibbs, H.K., Helkowski, J.H., Holloway, T., Howard,
511 E.A., Kucharik, C.J., Monfreda, C., Patz, J.A., Prentice, I.C., Ramankutty, N., &
512 Snyder, P.K. 2005. Global consequences of land use. *Science* 309: 570–574.
- 513 Gorham, E., Bayley, S.E., & Schindler, D.W. 1984. Ecological effects of acid
514 deposition upon peatlands: a neglected field in “acid-rain” research. *Can J Fish*
515 *Aquat Sci* 41:1256–1268.
- 516 Guillera-Arroita, G., Lahoz-Monfort, J.J., & Elith, J. 2014. Maxent is not a presence-
517 absence method: A comment on Thibaud et al. *Methods in Ecology and Evolution*
518 5: 1192–1197.
- 519 Hájková, P., Hájek, M., & Apostolova, I. 2006. Diversity of wetland vegetation in the
520 Bulgarian high mountains, main gradients and context-dependence of the pH role.
521 *Plant Ecology* 184: 111–130.
- 522 Hanski, I., Kuussaari, M., & Nieminen, M. 1994. Metapopulation structure and
523 migration in the butterfly *Melitaea cinxia*. *Ecology*, 75: 747–762.
- 524 He, F., & Hubbell, S.P. 2011. Species-area relationships always overestimate extinction
525 rates from habitat loss. *Nature* 473: 368–371.
- 526 Henle, K., Davies, K.F., Kleyer, M., Margules, C., & Settele, J. 2004. Predictors of
527 species sensitivity to fragmentation. *Biodiversity and Conservation* 13: 207–251.
- 528 Ibáñez, I., Katz, D.S.W., Peltier, D., Wolf, S.M., & Connor Barrie, B.T. 2014.
529 Assessing the integrated effects of landscape fragmentation on plants and plant
530 communities: The challenge of multiprocess-multiresponse dynamics. *Journal of*
531 *Ecology* 102: 882–895.

- 532 Jamin, A., Peintinger, M., Gimmi, U., Holderegger, R., & Bergamini, A. 2020.
533 Evidence for a possible extinction debt in Swiss wetland specialist plants. *Ecology*
534 *and Evolution* 10: 1264–1277.
- 535 Keil, P., Storch, D., & Jetz, W. 2015. On the decline of biodiversity due to area loss.
536 *Nature Communications* 6: 8837.
- 537 Koh, L.P., & Ghazoul, J. 2010. A matrix-calibrated species-area model for predicting
538 biodiversity losses due to land-use change. *Conservation Biology* 24: 994–1001.
- 539 Kudo, G., Kawai, Y., Amagai, Y., & Winkler, D.E. 2017. Degradation and recovery of
540 an alpine plant community: experimental removal of an encroaching dwarf
541 bamboo. *Alpine Botany* 127: 75–83.
- 542 Makishima, D., Sutou, R., Goto, A., Kawai, Y., Ishii, N., Taniguchi, H., Uchida, K.,
543 Shimazaki, M., Nakashizuka, T., Suyama, Y., Hikosaka, K., & Sasaki, T. 2021.
544 Potential extinction debt due to habitat loss and fragmentation in subalpine
545 moorland ecosystems. *Plant Ecology* 222: 445–457.
- 546 Manel, S., Williams, H.C., & Ormerod, S.J. 2001. Evaluating presence-absence models
547 in ecology: The need to account for prevalence. *Journal of Applied Ecology*,
548 38:921-931.
- 549 Merlin, A., Bonis, A., Damgaard, C.F., & Mesléard, F. 2015. Competition is a strong
550 driving factor in wetlands, peaking during drying out periods. *PLoS ONE* 10: 1–14.
- 551 Merow, C., Smith, M.J., & Silander, J.A. 2013. A practical guide to MaxEnt for
552 modeling species' distributions: What it does, and why inputs and settings matter.
553 *Ecography* 36: 1058–1069.
- 554 Noh, J. kyoungh, Echeverría, C., Pauchard, A., & Cuenca, P. 2019. Extinction debt in a
555 biodiversity hotspot: the case of the Chilean Winter Rainfall-Valdivian Forests.

- 556 *Landscape and Ecological Engineering* 15: 1–12.
- 557 Olsen, S.L., Evju, M., & Endrestøl, A. 2018. Fragmentation in calcareous grasslands:
558 species specialization matters. *Biodiversity and Conservation* 27: 2329–2361.
- 559 Pearce, J., & Ferrier, S. 2000. An evaluation of alternative algorithms for fitting species
560 distribution models using logistic regression. *Ecological Modelling* 128: 127–147.
- 561 Pereira, H.M., Leadley, P.W., Proença, V., Alkemade, R., Scharlemann, J.P.W.,
562 Fernandez-Manjarrés, J.F., Araújo, M.B., Balvanera, P., Biggs, R., Cheung,
563 W.W.L., Chini, L., Cooper, H.D., Gilman, E.L., Guénette, S., Hurtt, G.C.,
564 Huntington, H.P., Mace, G.M., Oberdorff, T., Revenga, C., Rodrigues, P., Scholes,
565 R.J., Sumaila, U.R., & Walpole, M. 2010. Scenarios for global biodiversity in the
566 21st century. *Science* 330: 1496–1501.
- 567 Phillips, S.B., Aneja, V.P., Kang, D., & Arya, S.P. 2006. Modelling and analysis of the
568 atmospheric nitrogen deposition in North Carolina. *International Journal of Global*
569 *Environmental Issues* 6: 231–252.
- 570 R Development Core Team. 2020. R: A language and environment for statistical
571 computing (ver. 4.0.3). R Foundation for Statistical Computing, Vienna.
- 572 Sasaki, T., Katabuchi, M., Kamiyama, C., Shimazaki, M., Nakashizuka, T., &
573 Hikosaka, K. 2012. Nestedness and niche-based species loss in moorland plant
574 communities. *Oikos* 121: 1783–1790.
- 575 Sasaki, T., Katabuchi, M., Kamiyama, C., Shimazaki, M., Nakashizuka, T., &
576 Hikosaka, K. 2013. Variations in species composition of moorland plant
577 communities along environmental gradients within a subalpine zone in northern
578 japan. *Wetlands* 33: 269–277.
- 579 Sasaki, T., Katabuchi, M., Kamiyama, C., Shimazaki, M., Nakashizuka, T., &

- 580 Hikosaka, K. 2014. Vulnerability of moorland plant communities to environmental
581 change: Consequences of realistic species loss on functional diversity. *Journal of*
582 *Applied Ecology* 51: 299–308.
- 583 Satake, Y., Hara, H., Watari, S., & Tominari, T. (eds) 1989. Wild flowers of Japan:
584 woody plants. Heibonsha, Tokyo, Japan (in Japanese)
- 585 Satake, Y., Ohwi, J., Kitamura, S., Watari, S., & Tominari, T. (eds) 1982. Wild flowers
586 of Japan: herbaceous plants. Heibonsha, Tokyo, Japan (in Japanese)
- 587 Shimazaki, M., Tsuyama, I., Nakazono, E., Nakao, K., Konoshima, M., Tanaka, N., &
588 Nakashizuka, T. 2012. Fine-resolution assessment of potential refugia for a
589 dominant fir species (*Abies mariesii*) of subalpine coniferous forests after climate
590 change. *Plant Ecology* 213: 603–612.
- 591 Stephanie, M., Ceri, W.H., & S.J., O. 2001. Evaluating presence – absence models in
592 ecology : the need to account for prevalence. *Journal of Applied Ecology* 38: 921–
593 931.
- 594 Wheeler, B.D., & Proctor, M.C.F. 2000. Ecological gradients, subdivisions and
595 terminology of north-west European mires. *Journal of Ecology* 88: 187–203.
- 596 Williams, H.M., Siegrist, J., & Wilson, A.M. 2021. Support for a relationship between
597 demography and modeled habitat suitability is scale dependent for the purple
598 martin Progne subis. *Journal of Animal Ecology* 90: 356–366.
- 599 Zhang, J., Nielsen, S.E., Chen, Y., Georges, D., Qin, Y., Wang, S.S., Svenning, J.C., &
600 Thuiller, W. 2017. Extinction risk of North American seed plants elevated by
601 climate and land-use change. *Journal of Applied Ecology* 54: 303–312.
- 602
- 603

Table 1. Elevation, grid size, number of grids, and environmental variables (data in each grid was averaged) at 19 moorland sites in the Hakkoda mountain range, Aomori Prefecture, northern Japan.

Site code	Elevation (m a.s.l.)	Grid size (m × m)	Number of grids	Environmental variables (mean)			
				pH	EC ($\mu\text{S cm}^{-1}$)	Soil moisture (%)	<i>Sphagnum</i> spp. cover (%)
Kamikenashi A	1217	40	40	3.74	62.29	97.00	20.67
Kamikenashi B	1164	40	72	3.71	82.48	86.34	10.19
Rope	908	20	32	3.92	110.17	71.76	73.49
Shimokenashi A	1047	40	45	4.41	71.04	73.25	24.08
Shimokenashi B	1034	40	32	4.14	61.7	84.15	36.26
Shimokenashi C	1022	40	27	4.00	65.29	71.94	11.4
Suiren A	988	20	11	4.49	151.58	64.29	23.91
Suiren B	986	20	9	4.63	276.3	73.53	4.41
Suiren C	964	20	8	4.19	133.96	78.52	47.00
Sukayu	893	20	13	3.86	155.33	93.17	93.21
Takada B	987	40	39	4.93	78.05	66.92	20.99

Takada C	1016	20	9	4.99	65.83	90.96	35.88
Takada D	1025	40	34	3.91	174.34	52.85	11.64
Takada G	1057	20	9	5.01	251.27	90.87	21.33
Takada I	1046	40	15	4.07	392.4	66.34	5.57
Tamoyachi A	1254	20	35	3.84	79.44	91.62	43.98
Tamoyachi B	1285	20	30	3.75	74.72	82.78	14.24
Tashiro	574	40	125	5.73	377.33	63.84	12.19
Yachi	774	40	39	4.77	137.68	99.81	49.49

Table 2. Selected species distribution model (SDM), number of predicted occurrences, accuracy rate, and AUC score for 30 species. Asterisks denote the 22 moorland specialists.

Species	Selected SDM	Number of predicted occurrences by SDM	Accuracy rate (%)	AUC
<i>Gaultheria adenostrix</i>	GLMM	17	87.9	0.923
<i>Nephrophyllidium crista-galli</i> *	GLMM	89	83.3	0.921
<i>Schizocodon soldanelloides</i>	GLMM	107	85.1	0.938
<i>Parnassia palustris</i> *	GLMM	187	73.3	0.860
<i>Menziesia multiflora</i> *	GLMM	5	92.8	0.923
<i>Carex omiana</i>	GLMM	164	82.5	0.913
<i>Nartheicum asiaticum</i> *	GLMM	184	79.9	0.914
<i>Platanthera tipuloides</i> *	GLMM	13	81.0	0.792
<i>Lobelia sessilifolia</i> *	GLMM	1	93.6	0.968
<i>Carex blepharicarpa</i>	GLMM	25	79.9	0.890
<i>Helonias orientalis</i> *	GLMM	1	79.1	0.784
<i>Hosta sieboldii</i> *	GLMM	136	92.4	0.974
<i>Sieversia pentapetala</i> *	GLMM	237	94.9	0.989
<i>Trientalis europaea</i>	GLMM	7	85.1	0.922
<i>Vaccinium oxycoccos</i> *	GLMM	549	75.4	0.874
<i>Ligularia hodgsonii</i>	GLMM	20	88.7	0.962
<i>Sanguisorba tenuifolia</i> *	GLMM	234	96.5	0.990
<i>Moliniopsis japonica</i> *	GLMM	622	93.3	0.946
<i>Ilex crenata</i> var. <i>paludosa</i>	GLMM	70	93.1	0.925
<i>Primula nipponica</i> *	GLMM	35	94.4	0.957

<i>Inula ciliaris</i> *	GLMM	1	93.1	0.970
<i>Carex michauxiana</i> *	GLMM	2	94.9	0.918
<i>Menyanthes trifoliata</i> *	GLMM	3	95.4	0.938
<i>Coptis trifolia</i> *	GLMM	3	85.4	0.887
<i>Rhynchospora yasudana</i> *	GLMM	288	72.7	0.853
<i>Drosera rotundifolia</i> *	GLMM	504	76.4	0.852
<i>Myrica gale</i> var. <i>tomentosa</i> *	GLMM	26	98.4	0.998
<i>Phragmites australis</i> *	GLMM	88	83.0	0.940
<i>Rhododendron japonicum</i>	GLMM	4	87.7	0.906
<i>Eriophorum vaginatum</i> *	GLMM	278	69.6	0.821

Table 3. Summary of the generalized linear model of the relationship between the relationship between the half-life of species richness (see Methods), and initial species richness (total number of species present before simulated area loss), averaged aggregation index across species (representing spatial patterns in species distributions), area, isolation, and elevation at each site.

Variables	Coefficient	SE	Z value	p value
(Intercept)	2.439	1.097	2.222	0.026
Initial species richness	-0.943	1.134	-0.832	0.405
Aggregation index across species	-0.163	1.094	-0.149	0.881
Area	0.661	2.241	0.295	0.768
Isolation	-0.451	1.000	-0.451	0.652
Elevation	-0.376	1.036	-0.363	0.717

Table 4. Summary of the generalized linear mixed-effects model of the relationship between the proportion of area lost leading to local extinction of each species, and aggregation index and occurrence rate (number of predicted occurrences divided by number of grids at each site) of each species at each site. Phylogenetic constraints were controlled by adding family as a random effect in the model.

Variables	Coefficient	SE	Z value	p value
(Intercept)	3.821	0.551	6.935	< 0.001
Aggregation index of each species	0.283	0.231	1.225	0.221
Occurrence rate of each species	3.610	0.776	4.653	< 0.001

Figure captions

Fig. 1. Distributions of eight species that are typically present in moorlands as predicted by the species distribution model at the Takada B site. Red grids indicate presence of the species. There was a spatial bias in the predicted distribution of each species.

Fig. 2. Spatial distribution of the likelihood of grid loss (a, d, g) and the predicted distribution of species richness for all species (b, e, h) and for moorland specialist (c, f, i) at the Tamoyachi A, Takada B, and Tashiro sites. The likelihood of grid loss is represented by the predicted LD values (see sections 2.4 and 2.6).

Fig. 3. Changes in species survival rate for all 30 species according to grid-based area loss simulations. Because area differed among grids, change trajectories of survival rate were plotted against the proportion of area lost. Green solid lines indicate change trajectories due to simulated grid-based area loss reflecting the actual area loss patterns, and green dashed lines indicate randomly simulated grid-based area loss. Green dashed lines are accompanied by gray shaded areas, indicating the 95% CIs for species loss trajectories by random area loss; however, the CIs are too narrow to visualize.

Fig. 4. Changes in species survival rate for 22 moorland specialists (Table 2) according to grid-based area loss simulations. Because area differed among grids, change trajectories of survival rate were plotted against the proportion of area lost. Blue solid lines indicate change trajectories due to simulated grid-based area loss reflecting the actual area loss patterns, and blue dashed lines indicate randomly simulated grid-based area loss. Blue dashed lines are

accompanied by gray shaded areas, indicating the 95% CIs for species loss trajectories by random area loss; however, the CIs are too narrow to visualize.

Fig. 5. Changes in species survival rate for 8 generalists (Table 2) according to grid-based area loss simulations. Because area differed among grids, change trajectories of survival rate were plotted against the proportion of area lost. Orange solid lines indicate change trajectories due to simulated grid-based area loss reflecting the actual area loss patterns, and orange dashed lines indicate randomly simulated grid-based area loss. Orange dashed lines are accompanied by gray shaded areas, indicating the 95% CIs for species loss trajectories by random area loss; however, the CIs are too narrow to visualize.

Fig. 6. Proportion of area lost leading to local extinction of each species across moorland sites. Here, area loss simulations were based on the realistic geometry of area loss. Species with orange boxplots are generalist species, and those with blue boxplots are moorland specialists.

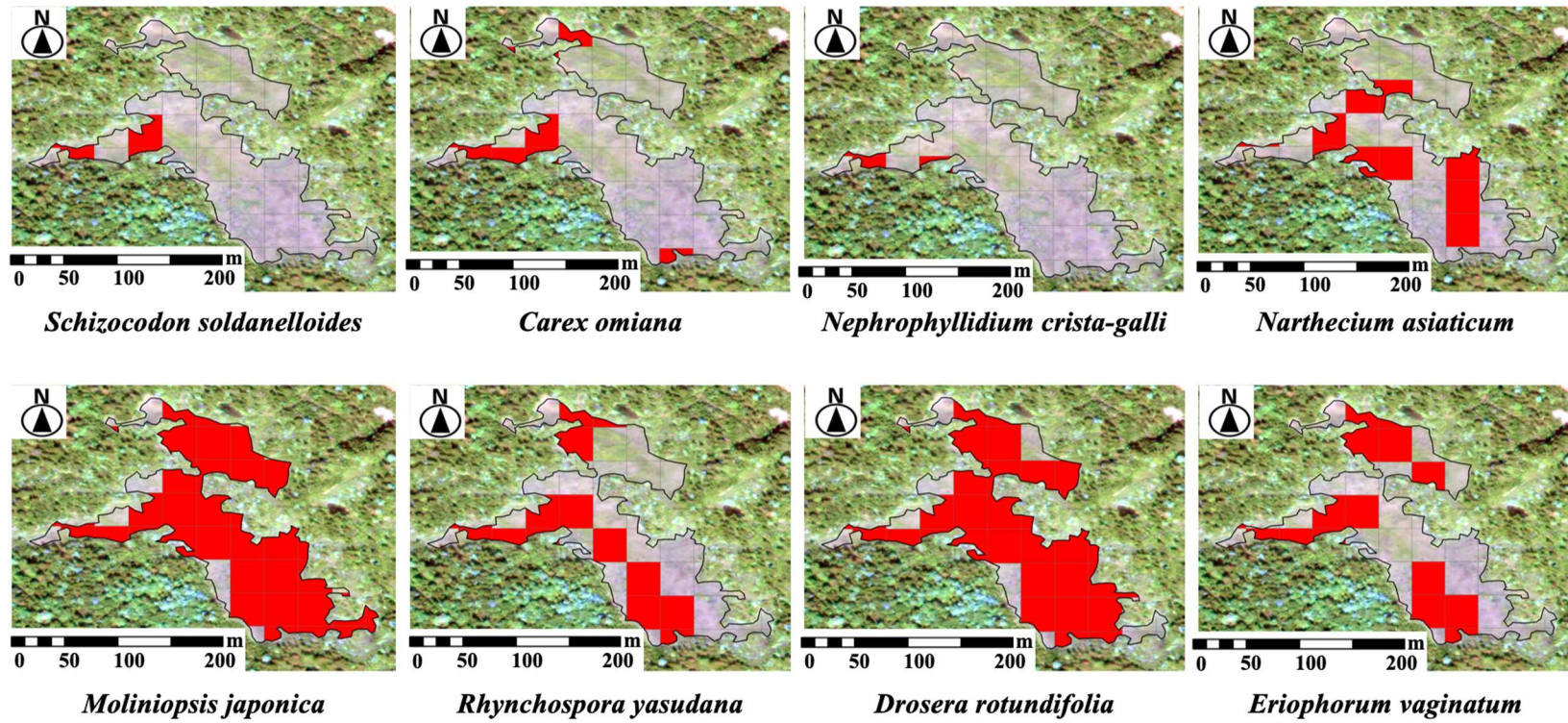


Fig. 1.

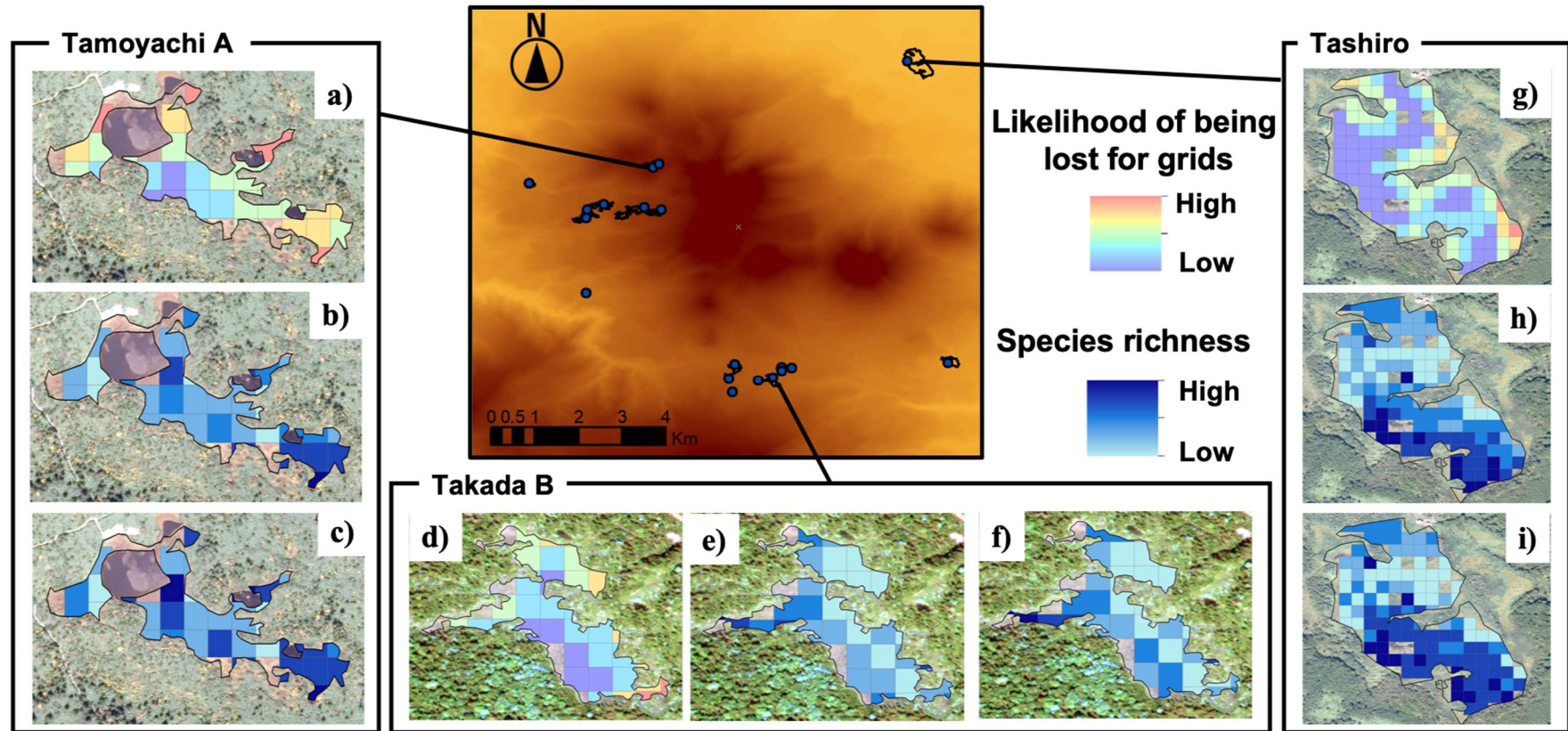


Fig. 2.

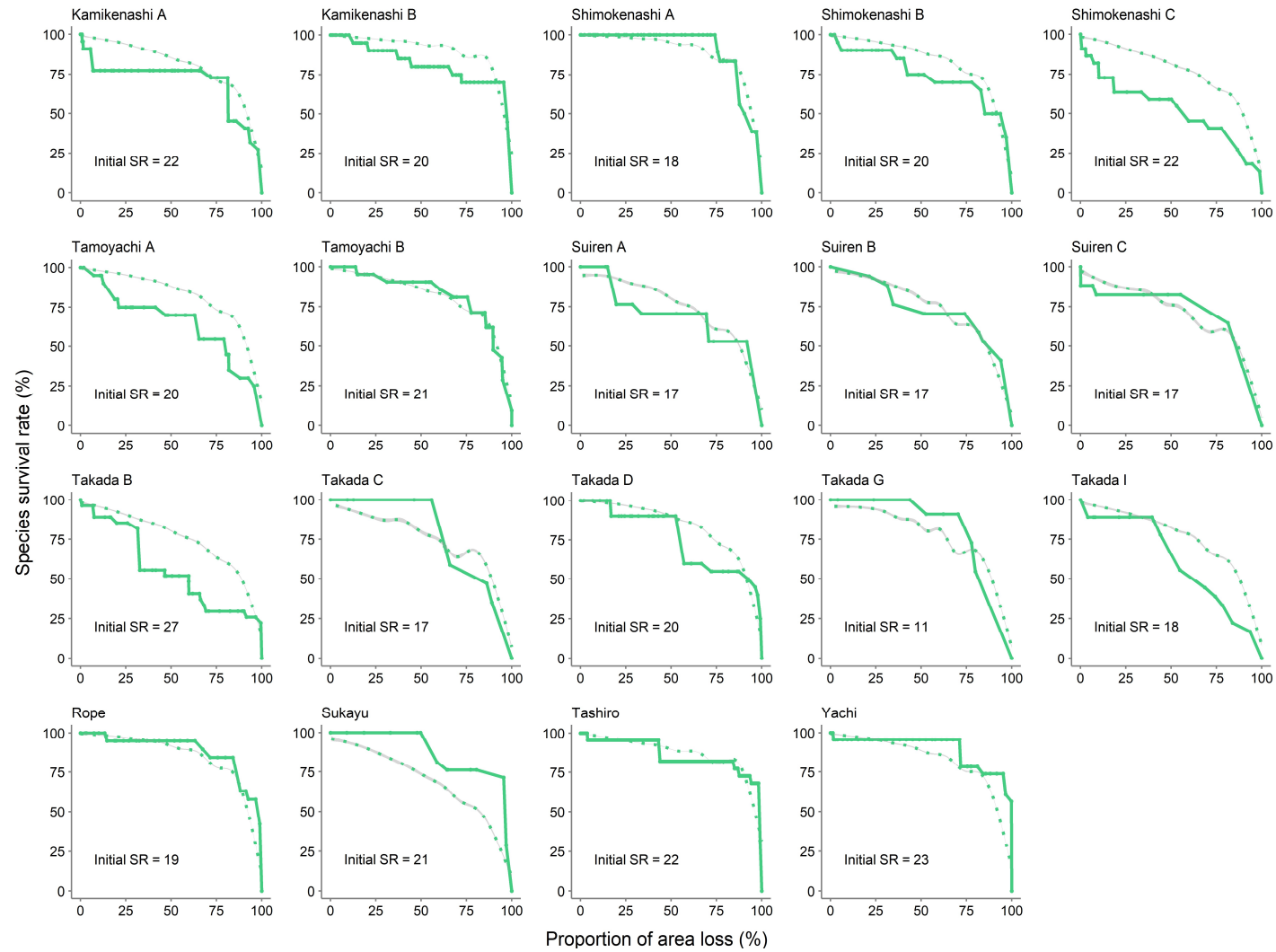


Fig. 3.

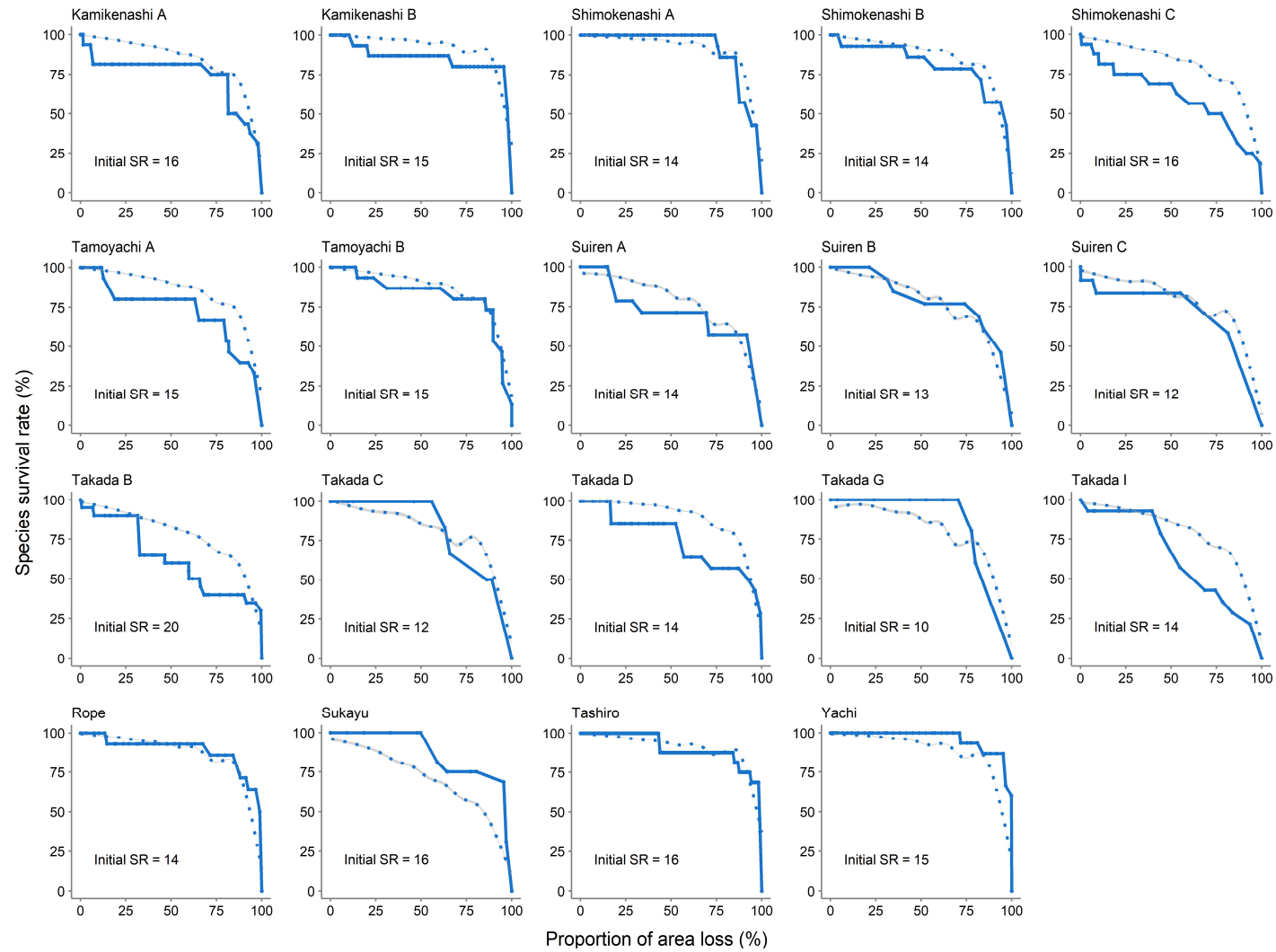


Fig. 4

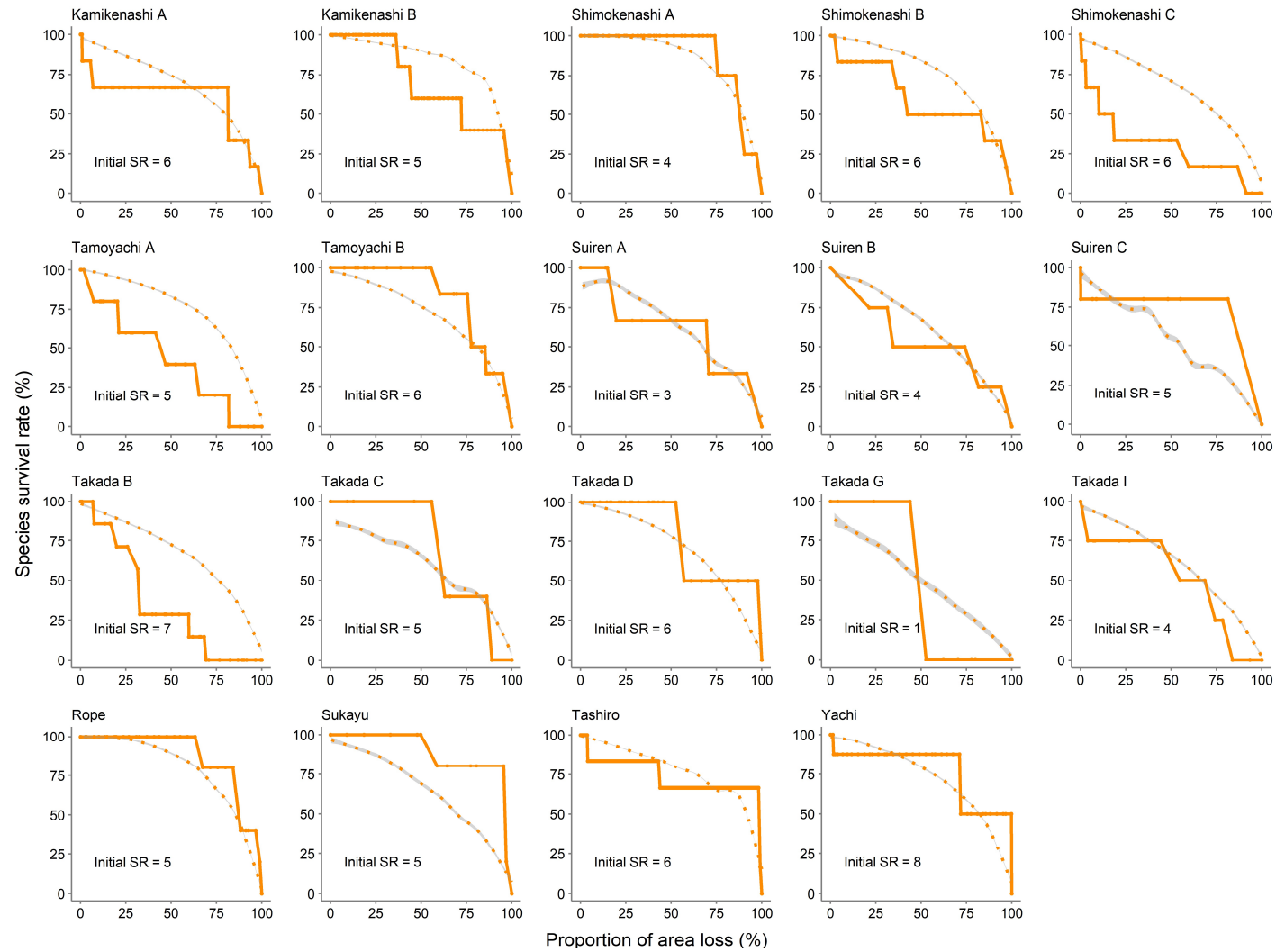


Fig. 5.

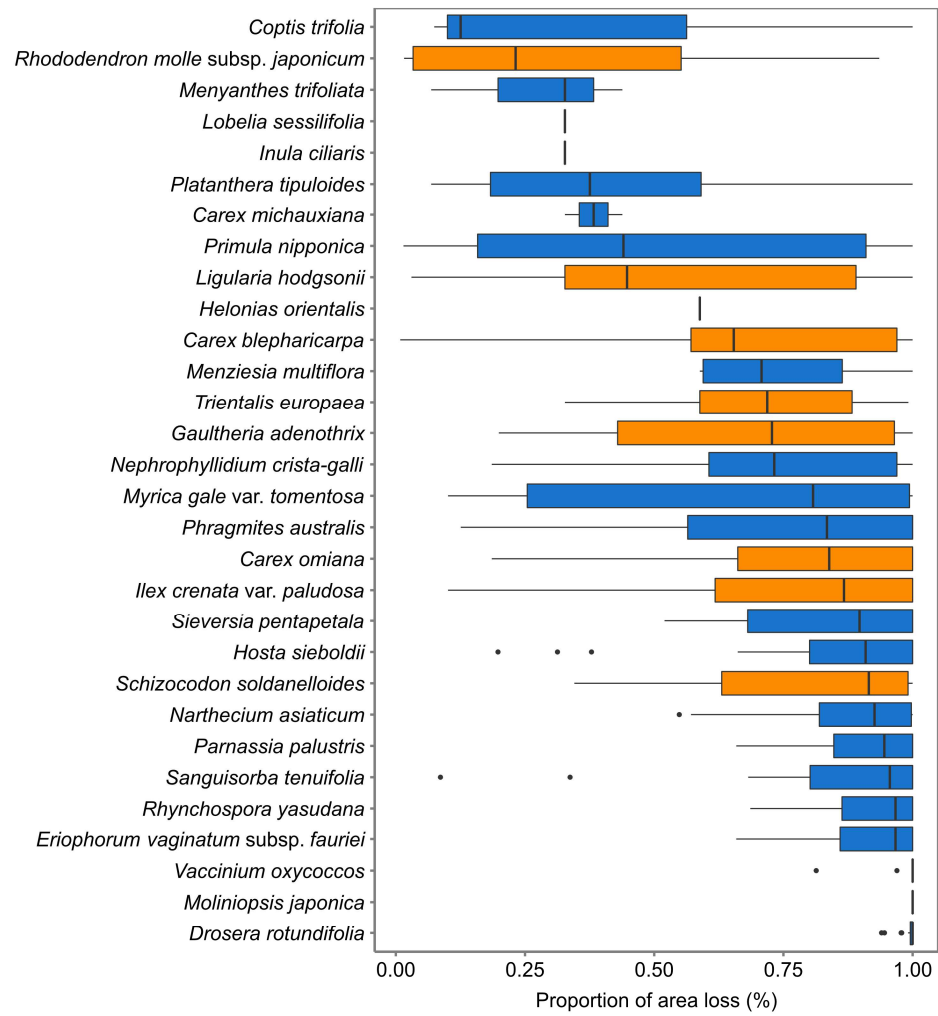


Fig. 6.